

# Evaluating influence of rainfall frequency and precipitation on landslide susceptibility: A case study in Lam Dong, Vietnam

NGUYEN Van Toan<sup>1\*</sup>, TRAN Dang An<sup>2</sup>, NGUYEN Van Hai<sup>2</sup>

<sup>1</sup> Faculty of Civil Engineering, Industrial University of Ho Chi Minh City, Ho Chi Minh City, Vietnam

<sup>2</sup> Thuyloi University Southern Campus, Vietnam

\* Corresponding email: [nguyenvantoan@iuh.edu.vn](mailto:nguyenvantoan@iuh.edu.vn)

**Abstract:** *Landslide susceptibility involves random topographical, geological, hydrological morphology, and hydrometeorology factors. Recent decades have seen alarming landslide hazards in Vietnam. Potential geological hazards subjected to extreme rainfall have threatened Vietnam's mountainous regions. This study evaluated the influence of rainfall on landslide susceptibility in Lam Dong province using machine learning algorithms coporated with the Analytic Hierarchy Process. Crucial impact factors were considered and analyzed in different rainfall scenarios. Landslide susceptibility maps developed correspond to frequency scenarios of antecedent rainfall data. The key findings revealed that rainfall conditions significantly influenced the landslide susceptibility in Lam Dong. The probability of rainfall-induced landslides could differ depending on the watershed due to rainfall behavior differences. The higher the rainfall intensity, the greater the risk of landslides. Steep hillsides of over 20% could be highly susceptible landslides to heavy rainfall intensity or more. Soil zones with high-complex slope conditions containing a high water content ratio and high swell index subjected to extreme rainfall could have a very high risk of landslides. Fuzzy probability could be a feasible tool to define crucial landslide-prone conditions regarding rainfall and slope and model the likelihood of landslide occurrence.*

**Keywords:** *Antecedent rainfall, Fuzzy probability, Landslide susceptibility, Machine learning algorithms, Rainfall intensity, Vietnam.*

## 1. Introduction

Recent efforts in landslide susceptibility analyzing and mapping approaches have evolved significantly, incorporating advances in remote sensing and GIS techniques, machine learning algorithms (MLA), big data analytics, and interdisciplinary approaches [1-20]. However, the challenge of studying landslide susceptibility has involved random or uncertain factors (i.e., topographical, geological, hydrological morphology, and hydrometeorology). In recent decades, Vietnam and the world have faced alarming landslides. Geohazards caused by heavy rainfall have significantly influenced Vietnam [10, 15-20].

Many factors could affect the landslide problem [1-12]. If based on factor stability over time, it could be grouped into two: (1) static/quasi-static factors and (2) dynamic/triggering factors (changing over a short period that may not follow the law). The main static/quasi-static factors include surface morphology, geological structure, stratigraphy, physical properties and behavior of the soil, and the hydraulic mechanism of the slope [7, 8]. In comparison, the main triggering factors include changes in weather and climate (affecting hydrodynamic conditions in the soil such as pore water pressure, water content, and saturation ratio); human activities (indirectly affecting geology or changing the topography and geomorphology, directly increasing the force component causing landslides); the influence of earthquakes; changes in natural morphology [21-23].

Previous works considered rainfall-induced slope instability in a changing environment [24-28]. Rain infiltration was the main component influencing slope stability [25-27]. The range of soil pore-water pressure changes widened with increasing rainfall intensity corresponding to the depth of rainfall infiltration [29]. However, rainfall intensity and amount per unit of time affected landslide risk, but not in the same way in areas with different natural conditions [15, 20, 30-37]. Nguyen et al. [19] applied the Analytic Hierarchy Process (AHP) to generate a landslide susceptibility index by considering eight major impact factors (i.e., slopes, aspect, land use, soil type, elevation, distance to road, distance to stream, and antecedent rainfall). Frequency scenarios using 3-day antecedent rainfall data following Regional Frequency Analysis (RFA) were taken into account. Rainfall antecedent conditions significantly influenced the susceptibility map of landslides (area under the curve, AUC > 70%) [19].

A few studies recommended that landslide susceptibility prediction modeling using event-driven landslide inventories has not been effective in the research area, independent of the landslide inventory map utilized for training and validation [38]. The impact of environmental change on landslide vulnerability should be investigated using a physical-based landslide forecasting model with rainfall episodes of different durations and intensities generated based on the climate-dependent rainfall intensity-duration-frequency (IDF) curves [39, 40]. Therefore, landslide risk assessment under multiple climate change scenarios could be room for advancement.

Recent efforts have long investigated relationships between rainfall and landslides, with analyzed proposals of models and significant advancement in knowledge of this field [19, 25, 41, 42]. The entire potential energy characteristic of the unsaturated soil slope was established by evaluating the real-time variations in system potential energy generated by rainwater penetration [25]. Rainfall infiltration's impacts on soil shear strength, self-weight of sliding mass, and seepage force were taken into consideration to show the relationship between the sliding depth of the failure surface and rainfall [25]. The slope slide was related to a characteristic traction development due to rain. Sun et al. evaluated the slope instability affected by rainwater through indoor model testing and simulation methods: change the law of water flow, dangerous sliding surface, seepage, and factor of safety over time under rainwater seepage [43]. However, these prior studies have not assessed the effects of rainfall intensity and cumulative rainfall on landslide risk.

This research presents a feasible approach to examining landslide susceptibility under rainfall frequency and precipitation impact using machine learning algorithms adapted to the AHP multicriteria decision-making method—first, a brief description of Lam Dong province (Vietnam) as the case study is presented. The following section introduces and illumines the methodology. Databases of key conditioning factors were built and analyzed, considering different rainfall scenarios. Next, spatial analyses were performed to predict landslide susceptibility. Finally, the key conclusions were drawn from the study.

## 2. Case study area

Lam Dong province is one part of the Central Highlands, Vietnam, having an area of approximately 9765 km<sup>2</sup> (Fig. 1). Lam Dong has a mountainous terrain, an average altitude of 200–1500m above sea level with loamy/weathered soil: mainly red basalt and alluvial soils (highly expansive)[44]. With this geological feature, the soil structure is weakened rapidly every time there is prolonged heavy rain, along with many hillside areas with relatively high slopes and areas with reduced vegetation cover. Therefore, the risk of landslides is always latent. Lam Dong had relatively large rainfall, although unevenly distributed throughout the year (the rainy season accounts for 85-90%, and the dry season accounts for 10-15%) in the rainy season from May to November [45].

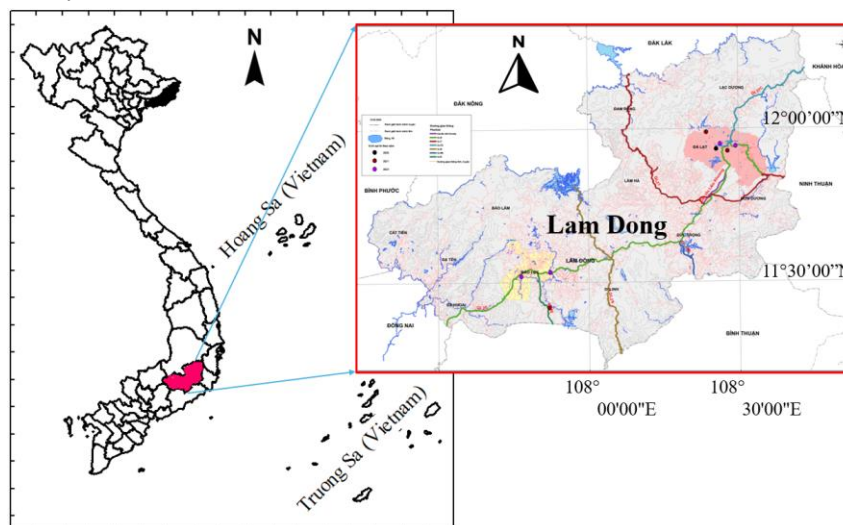
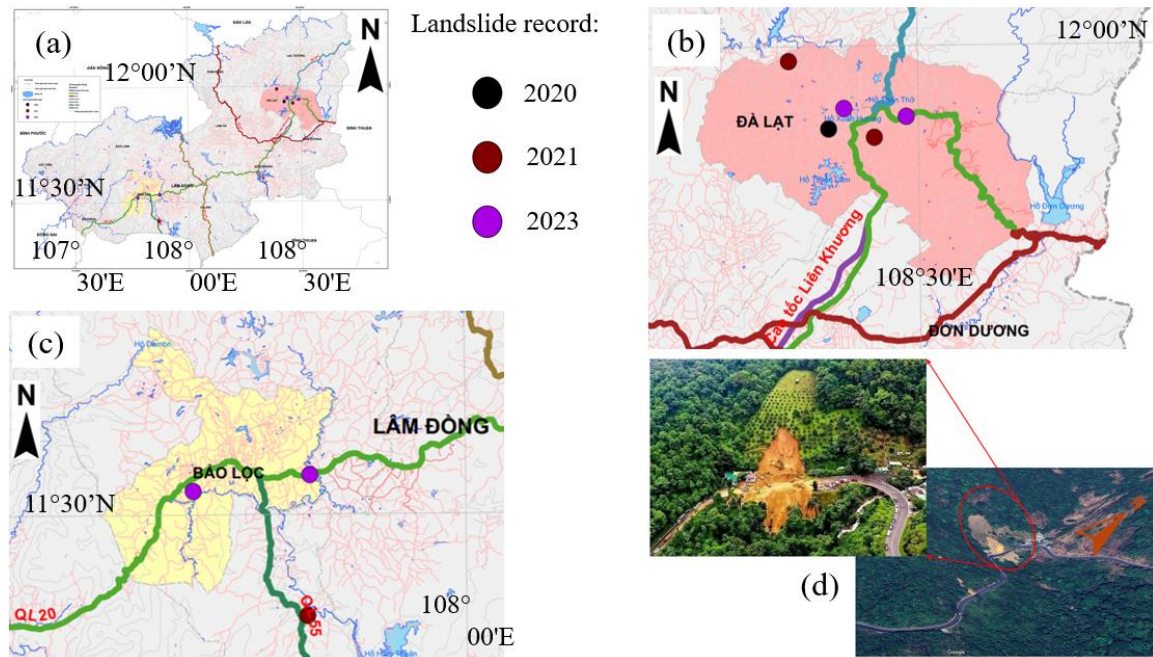


Fig. 1. Research area - Lam Dong province in the Vietnam Map

Landslides in Lam Dong province occur annually; however, in recent years, the landslides have become more complicated [44]. Notably, from June to July 2023, nearly 20 severe landslides occurred in Lam Dong province, killing nine people, according to a report [44]. On June 29, 2023, 13 landslides occurred in Da Lat City, killing two people and injuring three people; 3 houses were severely damaged, and nine houses were partially damaged. In July 2023, many landslides occurred: at Bao Loc Pass (in Da Huoi district), killing four people (see Fig. 2); the construction embankment in Da Lat city collapsed, causing two deaths. According to the People's Committee of Lam Dong province, in the first seven months of 2023,

the province recorded 13 heavy rains, causing 236 houses, seven bridges, four irrigation works, and two schools to be damaged, 336 hectares of crops were damaged [44, 45]. The general comment from researchers in the area was that prolonged heavy rains have been the primary trigger for the massive landslides [44, 45].



**Fig. 2.** Severe landslide records in recent years at Lam Dong: (a) whole province, (b) Da Lat city, and (c) Bao Loc city; (d) a serious landslide occurred in the middle of Bao Loc Pass, Lam Dong Province on July 30, 2023, killing four people [45]

### 3. Methodology

#### 3.1. Data Preparation

Digital elevation data with a grid size of 30×30m resolution utilized for numerical analyses was obtained from the digital elevation model (DEM) raster data of the Aster satellite (ASTERGDEMv2.0, USGS), as seen in Fig. 3. The topographic factors were derived from DEM data via ArcGIS software. The weathering crust and quaternary sediment of the Lam Dong region were referred to in the database of the Department of Geology and Minerals of Vietnam. Hydrological and geological data were obtained and digitized from the Vietnam National Geological Database. Landuse data was updated from the National and Provincial Database. Normalized difference vegetation index (NDVI) data was obtained from the Sentinel-2 remote sensing images. The digital database indicates that valley terrain is a lowland area distributed along the Da Nhim, Da Dang, Dai Binh, and Dong Nai rivers (in the districts of Don Duong, Lam Ha, Bao Loc, Cat Tien, and Da Teh): relatively flat with a slope of 0–3 degrees. The plateau terrain is mainly in Di Linh, Bao Lam (having an average altitude of more than 800 meters), and a hillslope of over 15 degrees (~27%).

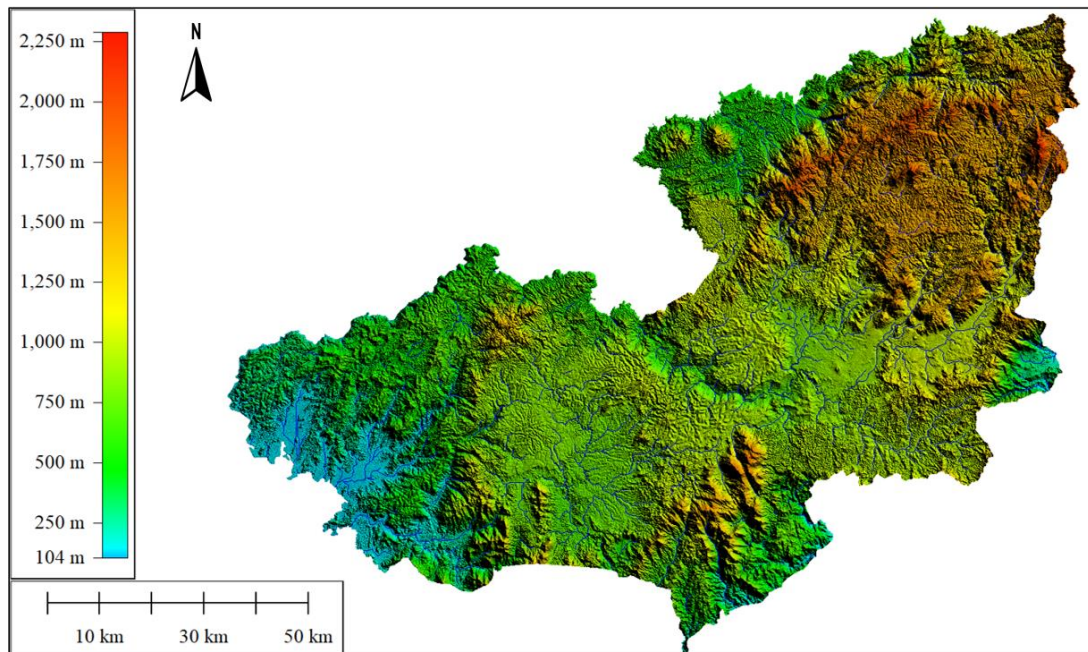


**Fig. 3.** DEM of Lam Dong Province for analyses

Rainfall frequency analyses were based on the 40-year rainfall database (from 1977 to 2019) of the 14 weather-monitoring stations of the Vietnam region-level Hydrology and Meteorology (national and province levels) and the Institute of Water Resources Planning (see Fig. 4). There was a relatively significant difference between regions in the province (the highest year reached ~2949 mm/year in the Bao Loc area; the lowest year reached ~1260 mm/year in Dai Ninh. In El Nino strong years (i.e., 1997–1998), rainfall was lower than the average for many years [45]. The total rainfall of the province was ~19.5 billion m<sup>3</sup>, in which the amount of water generating flow was ~11.0 billion m<sup>3</sup> (56.41%). The amount of infiltration and evaporation was ~8.5 billion m<sup>3</sup> (43.59%) [44].

Although the time series regressions were statistically credible, there remain doubts regarding the long-term 100-year extrapolation and geographical kriging. In addition, the rainfall frequency analysis assumes that the rainfall frequency behavior was independent of time, not counting any probable changes in the future. Therefore, rainfall intensity-duration-frequency (IDF) curves were generated based on the 40-year history record used for the current and predicted conditions of climate for a landslide-prone research region in Lam Dong province [45]. The IDFs were used to incorporate climate change impacts into the landslide modeling scenarios considering uncertainties in weather conditions. Assuming precipitation was obtained for Lam Dong province depending on the empirical reduction formula as Equation (1) (the Indian Meteorological Department proposed short intervals of 0.5, 1, 1.5, 2, 2.5, 3, 3.5, 4, 4.5, 5, 6, 12, and 24 hours, with return periods of 2, 5, 10, 25, 50, and 100 years) [39, 40]. The relationship between rainfall and short duration for the landslide-prone research region is shown in Fig. 5.

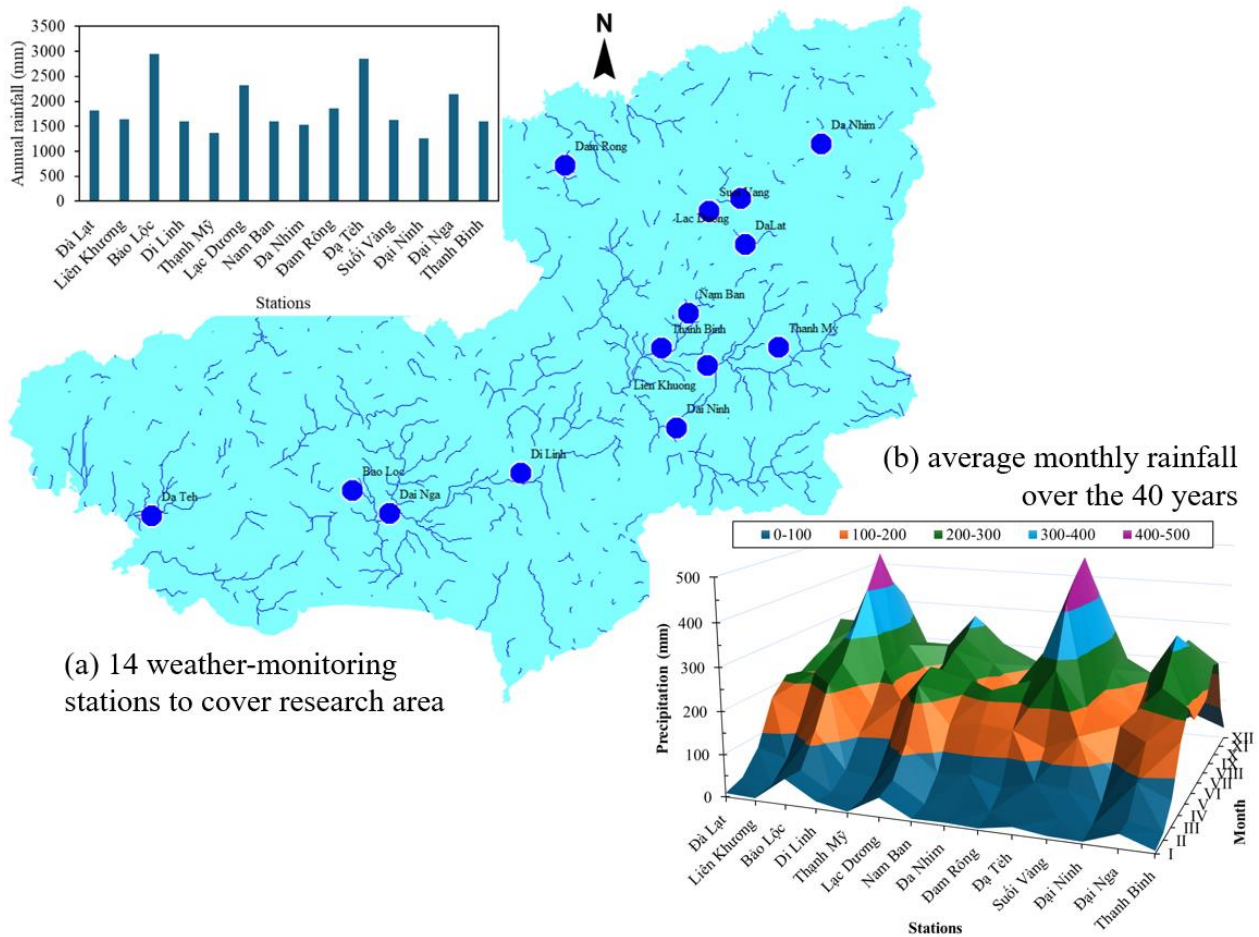


Fig. 4. Rainfall distribution characteristics in the study area from the 40-year rainfall database

$$P(t) = P(24) \times \left(\frac{t}{24}\right)^{1/3} \quad (1)$$

where  $P(24)$  is the value of daily precipitation (mm),  $P(t)$  is the desired depth of precipitation at the length of  $t$  hours (mm), and  $t$  is the rainfall duration (hour) when the depth of precipitation is necessary.

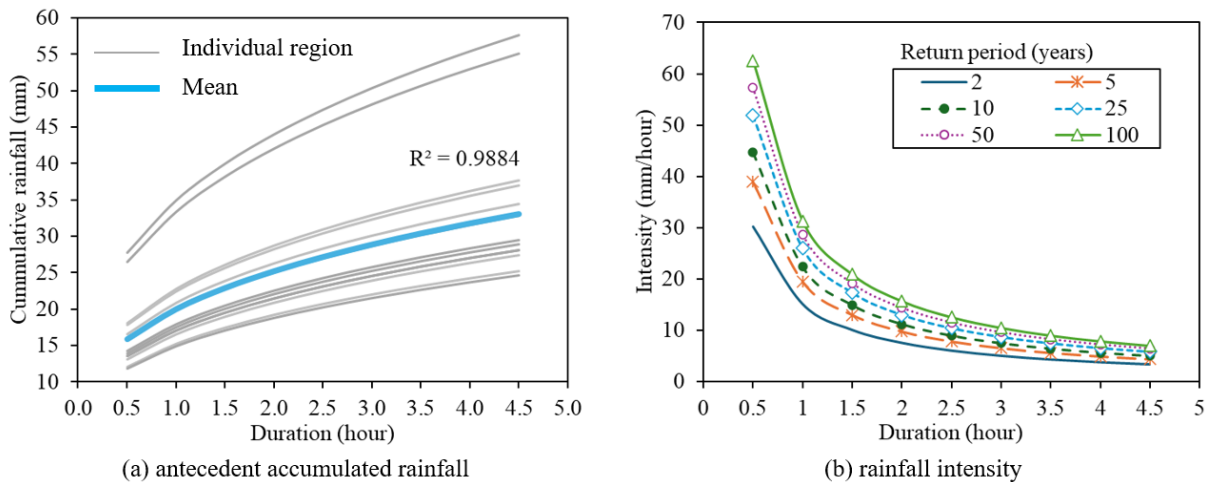
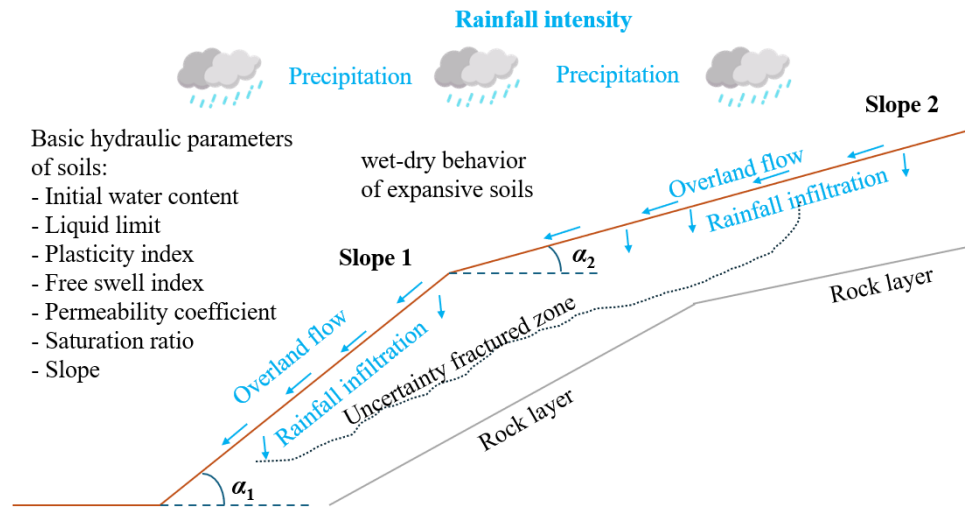


Fig. 5. Rainfall intensity-duration-frequency trending curves (IDF) for the landslide-prone research region

### 3.2. Landslide Susceptibility Mapping

A simplified mechanism model for the assessment of rainfall effect on slope instability was proposed in this study (see Fig. 6). The general limit equilibrium method can be expressed as Equation (2).

$$FOS = \frac{[\text{Sum of holding components}]}{[\text{Sum of sliding components}]} \quad (2)$$



**Fig. 6.** Simplified mechanism model for assessment of rainfall effect on slope instability

Many conditioning factors have been pointed out in landslide susceptibility studies [6, 14, 21, 46-50]. Understanding and determining the impact level of conditioning factors was critical in creating a high-precision landslide susceptibility model that influences computing landslides in the particular research area. Some recent studies have mentioned typical and key factors [9-12]. This current work conducted five conditioning factors representing and reflecting the essential characteristics of the research area (see Table 1). Inherent static and/or quasi-static factors acted as background conditions. While, dynamic factors acted as key triggering factors, in which rainfall intensity played an important role [20, 30, 37, 51]. Thus, rainfall intensity was used in this study to construct different research scenarios.

**Tab. 1.** Conditioning factors for landslide susceptibility analyses

| No. | Conditioning factors/ parameters                          | Type variable | Classification   | Category                |
|-----|---|---------------|--|-------------------------|
| 1   | Elevation (m)   | continuous    | (1) <100; (2) 100~200; (3) 200~500; (4) 500~1000; (5) 1000~1500; (6) 1500~2500; (7) >2500                | Topography              |
| 2   | Slope (degree)  | continuous    | (1) <5; (2) 5~15; (3) 15~25; (4) 25~35; (5) 35~45; (6) >45   | Topography              |
| 3   | Soil (geological structure of the crust) and its features | categorical   | (1) Clayey soils; (2) Loamy soils; (3) Sandy soils; (4) Gravel-sand mixtures; (5) Gravels                | Geology                 |
| 4   | Landuse/landcover (NDVI)                                  | continuous    | (1) <0; (2) 0~0.05; (3) 0.05~0.10; (4) 0.10~0.15; (5) 0.15~0.20; (6) 0.20~0.25; (7) 0.25~0.30; (8) >0.30 | Environment             |
| 5   | Rainfall intensity, $RI_{24hrs}$ (mm/24hours)             | continuous    | (1) <0.1; (2) 0.1~0.9; (3) 1.0~10; (4) 11~30; (5) 31~70; (6) 71~150; (7) >150                            | Hydrology & Meteorology |

The AHP has been well-known as a multicriteria decision-making approach based on pairwise comparisons to establish priority scales for LSM work [52-54], including assessments for highland regions in Vietnam [19]. A pairwise comparison matrix was created by rating each criterion against every other criterion on a relative dominant scale ranging from one to nine. The class with the least influence was assigned a value of one. In contrast, the class with the most significant impact was assigned a value of nine, indicating an increasing level of influence. The comparison matrices were constructed to determine the Consistency Ratio (CR) and Consistency Index (CI).

$$\text{Consistency Ratio (CR)} = \frac{\text{Consistency Index (CI)}}{\text{Random Index (RI)}} \quad (3)$$

$$\text{Consistency Index (CI)} = \frac{\lambda_{\max} - n}{n - 1} \quad (4)$$

where  $\lambda_{\max}$  is the matrix's largest or principal eigenvalue, which can be easily calculated from the matrix, and  $n$  is the matrix's order.

Following the assigned weightage, a factor map was categorized and incorporated into the GIS data. The acquisitive weights were merged with the several cause groups to yield landslide susceptibility indexes. The ROC (receiver operating characteristics) curve and AUC values were built for landslide susceptibility indexes. The simplified technique for carrying out this analysis was as follows: For  $n$  classes of landslide susceptibility indexes,  $n+1$  thresholds can be defined, with the first threshold value ( $i = 1$ ) less than the minimum susceptibility index observed in the most stable category and the last threshold value ( $i = n+1$ ) more significant than the maximum susceptibility index observed in the most sensitive category. In there, every threshold forms a confusion matrix in which four types of pixels are defined: true positive (TP), false positive (FP), true negative (TN), and false negative (FN) pixels. Simultaneously, two statistics could be calculated: true positive rate (TPR) and false positive rate (FPR). AUC value could be calculated based on the ROC curve when FPR and TPR were plotted on the X and Y axes, respectively.

$$\text{True Positive Rate (TPR)} = \frac{\text{True Positive (TP)}}{\text{True Positive (TP)} + \text{False Negative (FN)}} \quad (5)$$

$$\text{False Positive Rate (FPR)} = \frac{\text{False Positive (FP)}}{\text{True Negative (TN)} + \text{False Positive (FP)}} \quad (6)$$

$$\text{AUC} = \sum_{i=2}^{n+1} \frac{1}{2} \sqrt{(x_i - x_{i+1})^2} \times (y_i + y_{i+1}) \quad (7)$$

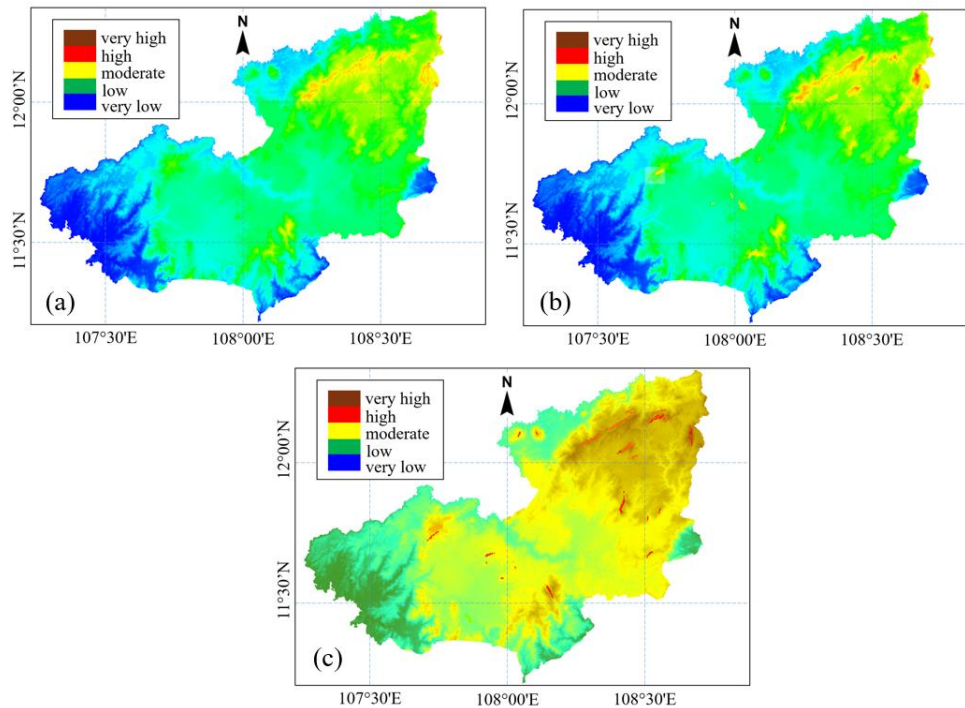
Landslide susceptibility maps were achieved from spatial analyses using MLA and adapting AHP [as generalized in Equation (8)]. Conditioning factors were reclassified and weighted based on their contribution to landslide susceptibility factors (aka landslide susceptibility indexes) to reflect different risk levels for landslide susceptibility. The AUC-ROC analysis was adopted to validate the analyzed results of predicted susceptibility zones by comparing them with observed data and known landslide locations from the landslide records [45].

$$\text{Raster dataset} = \sum_i [\text{var}]_i \times [w]_i \quad (8)$$

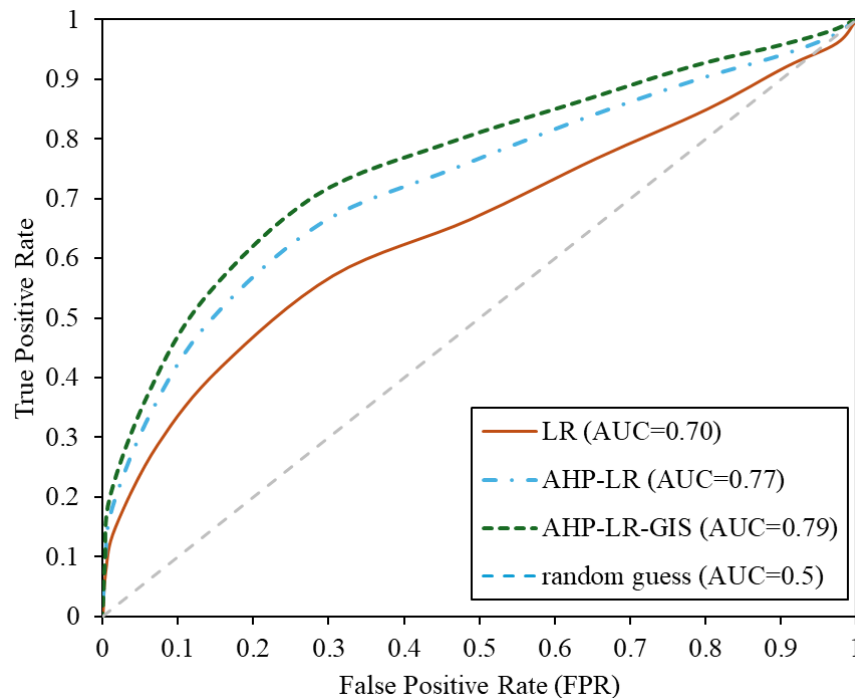
#### 4. Results and Discussion

Fig. 7 shows variations in expected susceptibility levels based on rainfall intensity and duration. The AUC of logistic regression analysis was adopted to examine the landslide susceptibility prediction results. The computed AUC was higher than 0.7, indicating that all conditioning factors produced acceptable outcomes in the landslide susceptibility analysis for Lam Dong province (see Fig. 8). Fig. 8 illustrates the ROC charts of landslide susceptibility models considering multivariate logistic regression (LR), AHP and GIS-data. In terms of overall performance, the stacking model AHP-LR-GIS outperformed the other landslide models (AUC = 0.79), followed by AHP-LR (0.77) and individual LR (0.70). The hybrid analysis model based on collaboration between the AHP, LR, and GIS considerably enhanced single techniques for calculating AUC. Several prior studies have advised adopting integrated approaches [55, 56].

Generally, most of the study area was at moderate or lower landslide risk level under the impact of light rainfall. In steep slope areas, the risk of landslides increased significantly and became more widespread with moderate rainfall intensity. Meanwhile, there was a significant change in the level of landslide risk when affected by heavy rainfall intensity or more. These studied results were quite consistent with the assessment reports [17, 44]. Landslides have been historically recorded to occur annually between June and October (in the rainy season). In the rainy season, landslides often occur on mountain passes through steep hills such as National Highways 20, 27, and 28 [44].



**Fig. 7.** Variations of predicted landslide susceptibility levels to the rainfall intensities and durations: (a) light rainfall ( $RI_{24hrs} \leq 20\text{mm}$ ); (b) moderate rainfall ( $RI_{24hrs} = 20\text{--}50\text{mm}$ ); and (c) heavy rainfall ( $RI_{24hrs} \geq 50\text{mm}$ )



**Fig. 8.** ROC curves for evaluation of landslide susceptibility models

For high mountainous areas, landslides were recorded at upstream rivers (Lac Duong, Don Duong, and Di Linh districts) due to steep terrain (slope > 20%) and high surface weathering. In addition, landslides occurred in urban areas, especially Da Lat city (moderate slope > 15%), because the city area had a high probability of medium or higher rainfall intensity. Although rainfall was more concentrated in the Southwest region (Da Teh - Bao Loc - Dai Nga) of Lam Dong province (see Fig. 4), the Lac Duong - Da Lat region was at high risk of landslides. In particular, landslides due to geological disasters occurred seriously in the Di Linh district.

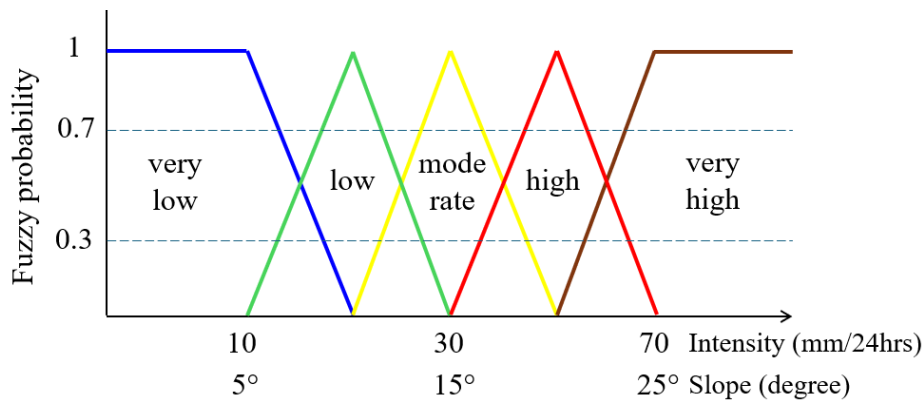


**Fig. 9.** Schematic of proposed fuzzy logic to define pivotal landslide-prone conditions (i.e., rainfall and slope) and probability could model the likelihood of landslide occurrence for Lam Dong province.

The previous precipitation and soil moisture levels were most critical for the initial stage of landslides [20, 24, 28, 35, 43]. Fuzzy probabilities could define uncertain events in landslide susceptibility mapping that require statistical and qualitative assessments [57]. A fuzzy logic schematic was proposed to define crucial landslide-prone conditions (i.e., rainfall and slope), and probability could model the likelihood of landslide occurrence for Lam Dong province (see Fig. 9). Using antecedent rainfall measurements was a key difficulty in predicting landslide occurrence, which related to the duration over which the accumulation of precipitation. Thus, there was a considerable scatter in the considered timeframes from prior studies, as shown in Table 2 [58–60]. Long-duration (days) and short-duration precipitation (hours) are crucial time triggers for shallow landslides because the critical short-duration rainfall intensity decreased as the antecedent accumulated rainfall increased [28]. This work considered rainfall thresholds initiating landslides based on analyses of landslide records within the research scope and location. This proposal was similar to law landslide rainfall thresholds in the neighboring regions with short-duration antecedent precipitation [20, 24, 35, 43].

**Tab. 2.** Rainfall and intensity thresholds initiating landslides

| No. | Region            | Rainfall thresholds initiating landslides<br>(A = accumulated rainfall days;<br>$RI_{24hrs}$ = 24-hour rainfall)  | Intensity thresholds initiating landslides<br>(I = hourly rainfall intensity; D = rainfall duration) | Ref.      |
|-----|-------------------|---|--|-----------|
| 1   | China             | NA  | $I = 49.11 - 6.81 \times D$<br>$1 < D < 5$ (hours)   | [58]      |
| 2   | Hong Kong         | Minor: $A_{15days} > 50$ mm & $RI_{24hrs} > 50$ mm<br>Severe: $A_{15days} > 200$ mm & $RI_{24hrs} > 100$ mm<br>Very severe: $A_{15days} > 350$ mm & $RI_{24hrs} > 100$ mm | $I = 41.83 \times D^{-0.58}$<br>$1 < D < 12$ (hours)   | [58, 59]  |
| 3   | Japan             | $RI_{24hrs} > 200$ mm   | $I = 39.71 \times D^{-0.62}$<br>$0.5 < D < 12$ (hours)   | [58, 61]  |
| 4   | Indonesia         | NA  | $I = 92.06 - 10.68 \times D$<br>$2 < D < 4$ (hours)  | [58]      |
| 5   | Sri Lanka         | $A_{3days} > 200$ mm<br>Low probability, mean annual precipitation: $A_{MAP} < 0.05$  | NA   | [60]      |
| 6   | Lam Dong, Vietnam | Moderate: $RI_{24hrs} > 30$ mm<br>Severe: $RI_{24hrs} > 70$ mm  | $I = 22.46 - 5.18 \times D$<br>$0.5 < D < 4$ (hours)   | This work |

## 5. Conclusions

The predicted landslide susceptibility level was evaluated by rainfall frequency and precipitation in Lam Dong province. A feasible approach to examining landslide susceptibility analysis using machine learning algorithms adapted to the Analytic Hierarchy Process (AHP) multicriteria decision-making method was presented. The pivotal findings of this study can be obtained as follows:

(1) Rainfall significantly affected the landslide susceptibility in Lam Dong province. The higher the rain intensity, the greater the risk of landslides. Most of the research area could be at moderate or lower landslide risk levels under the impact of light rainfall.

(2) The steep hills were significantly sensitive to heavy rainfall intensity. Da Lat City had a high potential for landslides due to the high probability of heavy rain intensity despite its moderate slope. Rainfall-induced landslide levels could vary depending on the watershed due to changes in rainfall behavior. Steep hillsides greater than 20% or more could be vulnerable landslides to severe rainfall.

(3) Fuzzy probabilities could be used to define crucial landslide-prone conditions, especially rainfall and slope, and model the likelihood of landslide occurrence for Lam Dong province. Antecedent precipitation (accumulative rainfall) with short-duration precipitation could considerably trigger shallow landslides in strong weathering geological conditions; the soil has high swelling properties.

More studies in landslide susceptibility, especially based on empirical modeling systems, could make room for future work to assess landslide risk in Lam Dong province in detail and comprehensively.

## Acknowledgements

This research received no specific grant from any funding agency in the public, commercial, or not-for-profit sectors.

## Literature - References

1. Mohan A, Singh AK, Kumar B, Dwivedi R. Review on remote sensing methods for landslide detection using machine and deep learning. *Transactions on Emerging Telecommunications Technologies* 2021;32:e3998. <https://doi.org/10.1002/ett.3998>.
2. Chowdhury MS. A review on landslide susceptibility mapping research in Bangladesh. *Heliyon* 2023;9:e17972. <https://doi.org/10.1016/j.heliyon.2023.e17972>.
3. Hemasinghe H, Rangali RSS, Deshapriya NL, Samarakoon L. Landslide susceptibility mapping using logistic regression model (a case study in Badulla District, Sri Lanka). *Procedia Engineering* 2018;212:1046-53. <https://doi.org/10.1016/j.proeng.2018.01.135>.
4. Boussouf S, Fernández T, Hart AB. Landslide susceptibility mapping using maximum entropy (MaxEnt) and geographically weighted logistic regression (GWLRL) models in the Río Aguas catchment (Almería, SE Spain). *Natural Hazards* 2023;117:207-35. <https://doi.org/10.1007/s11069-023-05857-7>.
5. Małka A. Landslide susceptibility mapping of Gdynia using geographic information system-based statistical models. *Natural Hazards* 2021;107:639-74. <https://doi.org/10.1007/s11069-021-04599-8>.
6. Spiekermann RI, McColl S, Fuller I, Dymond J, Burkitt L, Smith HG. Quantifying the influence of individual trees on slope stability at landscape scale. *Journal of Environmental Management* 2021;286:112194. <https://doi.org/10.1016/j.jenvman.2021.112194>.
7. Gerzsenyi D, Albert G. Landslide inventory validation and susceptibility mapping in the Gerecse Hills, Hungary. *Geo-spatial Information Science* 2021;24:498-508. <https://doi.org/10.1080/10095020.2020.1870872>.
8. Huang Y, Zhao L. Review on landslide susceptibility mapping using support vector machines. *CATENA* 2018;165:520-9. <https://doi.org/10.1016/j.catena.2018.03.003>.
9. Agboola G, Beni LH, Elbayoumi T, Thompson G. Optimizing landslide susceptibility mapping using machine learning and geospatial techniques. *Ecological Informatics* 2024;81:102583. <https://doi.org/10.1016/j.ecoinf.2024.102583>.
10. Thanh TPT, Thu HLT, Ngoc PV, Ngoc PV. Application of the GIS and R program for landslide susceptibility mapping: A case study in Van Yen, Yen Bai, Vietnam. *Journal of Science on Natural Resources and Environment* 2022:104-13. <https://vjol.info.vn/index.php/hunre/article/view/74506>.
11. Trinh T, Luu BT, Le THT, Nguyen DH, Van Tran T, Van Nguyen TH, et al. A comparative analysis of weight-based machine learning methods for landslide susceptibility mapping in Ha Giang area. *Big Earth Data* 2023;7:1005-34. <https://doi.org/10.1080/20964471.2022.2043520>.

12. Ado M, Amitab K, Maji AK, Jasińska E, Gono R, Leonowicz Z, et al. Landslide Susceptibility Mapping Using Machine Learning: A Literature Survey. *Remote Sensing* 2022. <https://doi.org/10.3390/rs14133029>.
13. Manan WAA, Rashid ASA, Abdul Rahman MZA, Khanan MFA. Assessment on Recent Landslide Susceptibility Mapping Methods: A Review. *IOP Conference Series: Earth and Environmental Science* 2022;971:012032. <https://doi.org/10.1088/1755-1315/971/1/012032>.
14. Peng L, Niu R, Huang B, Wu X, Zhao Y, Ye R. Landslide susceptibility mapping based on rough set theory and support vector machines: A case of the Three Gorges area, China. *Geomorphology* 2014;204:287-301. <https://doi.org/10.1016/j.geomorph.2013.08.013>.
15. Thanh LN, De Smedt F. Slope stability analysis using a physically based model: a case study from A Luoi district in Thua Thien-Hue Province, Vietnam. *Landslides* 2014;11:897-907. <https://doi.org/10.1007/s10346-013-0437-x>.
16. JICA B. Natural Disaster Risk Assessment and Area Business Continuity Plan Formulation for Industrial Agglomerated Areas in the ASEAN Region - Country Report Vietnam. AHA Centre, Japan International Cooperation Agency: JICA; 2015. <https://openjicareport.jica.go.jp/pdf/1000023398.pdf>.
17. Thanh DQ, Nguyen DH, Prakash I, Jaafari A, Nguyen VT, Phong TV, et al. GIS based frequency ratio method for landslide susceptibility mapping at Da Lat City, Lam Dong province, Vietnam. *Vietnam Journal of Earth Sciences* 2020;42:55-66. <https://doi.org/10.15625/0866-7187/42/1/14758>.
18. Tuan TA, Tam TT, Hong PV, Nguyet NTA. Landslide susceptibility mapping based on the Weights of Evidence model for mountainous areas of Quang Nam province, Vietnam. *Journal of Hydro-meteorology* 2023;31-45. [https://doi.org/10.36335/VNJHM.2023\(17\).31-45](https://doi.org/10.36335/VNJHM.2023(17).31-45)
19. Nguyen CC, Vo P, Doan VL, Nguyen QB, Nguyen TC, Nguyen QD. Assessment of the Effects of Rainfall Frequency on Landslide Susceptibility Mapping Using AHP Method: A Case Study for a Mountainous Region in Central Vietnam. In: Alcántara-Ayala I, Arbanas Ž, Huntley D, Konagai K, Mikoš M, Sassa K, et al., editors. *Progress in Landslide Research and Technology*, Volume 1 Issue 2, 2022. Cham: Springer International Publishing; 2023. p. 87-98. 10.1007/978-3-031-18471-0\_7.
20. Doan VL, Nguyen B-Q-V, Nguyen CC, Nguyen CT. Effect of time-variant rainfall on landslide susceptibility: A case study in Quang Ngai Province, Vietnam. *Vietnam Journal of Earth Sciences* 2024;46:202-20. <https://doi.org/10.15625/2615-9783/20065>.
21. Van-Toan N. Numerical modeling of Probabilistic slope stability Analysis on GeoStudio. *Journal of Water Resources & Environmental Engineering* 2016;55:167-73. <https://vjol.info.vn/index.php/DHTL/article/view/30461>.
22. Sonker I, Tripathi JN, Swarnim. Remote sensing and GIS-based landslide susceptibility mapping using frequency ratio method in Sikkim Himalaya. *Quaternary Science Advances* 2022;8:100067. <https://doi.org/10.1016/j.qsa.2022.100067>.
23. Goyes-Peñañiel P, Hernandez-Rojas A. Landslide susceptibility index based on the integration of logistic regression and weights of evidence: A case study in Popayan, Colombia. *Engineering Geology* 2021;280:105958. <https://doi.org/10.1016/j.enggeo.2020.105958>.
24. Robinson JD, Vahedifard F, AghaKouchak A. Rainfall-triggered slope instabilities under a changing climate: comparative study using historical and projected precipitation extremes. *Canadian Geotechnical Journal* 2016;54:117-27. <https://doi.org/10.1139/cgj-2015-0602>.
25. Fang W, You R, Hou H, Sun J, Yu T. Slope stability analysis under rainfall infiltration condition using the minimum potential energy method. *Archives of Civil and Mechanical Engineering* 2023;23:117. <https://doi.org/10.1007/s43452-023-00660-4>.
26. Zhao Y, Zhang H, Wang G, Yang Y, Tian W. Analysis of Slope Stability Based on Layered Infiltration Theory under Wet-dry Cycle Conditions. *KSCE Journal of Civil Engineering* 2024:100028. <https://doi.org/10.1016/j.kscej.2024.100028>.
27. Li X, Liu X, Liu Y, Yang Z, Zhang L. Probabilistic slope stability analysis considering the non-stationary and spatially variable permeability under rainfall infiltration-redistribution. *Bulletin of Engineering Geology and the Environment* 2023;82:350. <https://doi.org/10.1007/s10064-023-03351-9>.
28. Gonzalez FCG, Cavacanti MdCR, Nahas Ribeiro W, Mendonça MBd, Haddad AN. A systematic review on rainfall thresholds for landslides occurrence. *Heliyon* 2024;10:e23247. <https://doi.org/10.1016/j.heliyon.2023.e23247>.
29. Tao G, Feng S, Xiao H, Gu K, Wu Z. Rainfall Infiltration Test and Numerical Simulation Analysis of a Large Unsaturated Soil Slope. *Journal of Hydrologic Engineering* 2024;29:04024020. <https://doi.org/10.1061/JHYEFF.HEENG-6190>.

30. Maragaño-Carmona G, Fustos Toribio IJ, Descote P-Y, Robledo LF, Villalobos D, Gatica G. Rainfall-Induced Landslide Assessment under Different Precipitation Thresholds Using Remote Sensing Data: A Central Andes Case. *Water*2023. <https://doi.org/10.3390/w15142514>.
31. [31] Huang F, Teng Z, Guo Z, Catani F, Huang J. Uncertainties of landslide susceptibility prediction: Influences of different spatial resolutions, machine learning models and proportions of training and testing dataset. *Rock Mechanics Bulletin* 2023;2:100028. <https://doi.org/10.1016/j.rockmb.2023.100028>.
32. Huang ML, Sun DA, Wang CH, Keleta Y. Reliability analysis of unsaturated soil slope stability using spatial random field-based Bayesian method. *Landslides* 2021;18:1177-89. <https://doi.org/10.1007/s10346-020-01525-0>.
33. Chan H-C, Chen P-A, Lee J-T. Rainfall-Induced Landslide Susceptibility Using a Rainfall–Runoff Model and Logistic Regression. *Water*2018. <https://doi.org/10.3390/w10101354>.
34. Oguz EA, Benestad RE, Parding KM, Depina I, Thakur V. Quantification of climate change impact on rainfall-induced shallow landslide susceptibility: a case study in central Norway. *Georisk: Assessment and Management of Risk for Engineered Systems and Geohazards* 2024;18:467-90. <https://doi.org/10.1080/17499518.2023.2283848>.
35. Teja TS, Dikshit A, Satyam N. Determination of Rainfall Thresholds for Landslide Prediction Using an Algorithm-Based Approach: Case Study in the Darjeeling Himalayas, India. *Geosciences*2019. <https://doi.org/10.3390/geosciences9070302>.
36. D’Ippolito A, Lupiano V, Rago V, Terranova OG, Iovine G. Triggering of Rain-Induced Landslides, with Applications in Southern Italy. *Water*2023. <https://doi.org/10.3390/w15020277>.
37. Kimura T, Sato G, Ozaki T, Van Thang N, Wakai A. Land Cover Trajectories and Their Impacts on Rainfall-Triggered Landslide Occurrence in a Cultivated Mountainous Region of Western Japan. *Water*2023. <https://doi.org/10.3390/w15244211>.
38. Oliveira SC, Zêzere JL, Garcia RAC, Pereira S, Vaz T, Melo R. Landslide susceptibility assessment using different rainfall event-based landslide inventories: advantages and limitations. *Natural Hazards* 2024;120:9361-99. <https://doi.org/10.1007/s11069-024-06691-1>.
39. Shamkhi MS, Azeez MK, Obeid ZH. Deriving rainfall intensity–duration–frequency (IDF) curves and testing the best distribution using EasyFit software 5.5 for Kut city, Iraq. *Open Engineering* 2022;12:834-43. <https://doi.org/10.1515/eng-2022-0330>.
40. Mohammed A, Dan’Azumi S, Modibbo AA, Adamu AA. Development of Rainfall Intensity Duration Frequency (IDF) Curves for Design of Hydraulic Structures in Kano State, Nigeria. *Platform-A Journal of Engineering* 2021;5:10-22.
41. Zhang L, Tang X, Yang J. Rainfall-induced flowslides of granular soil slopes: Insights from grain-scale modeling. *Engineering Geology* 2023;323:107223. <https://doi.org/10.1016/j.enggeo.2023.107223>.
42. Thomas J, Gupta M, Srivastava PK, Petropoulos GP. Assessment of a Dynamic Physically Based Slope Stability Model to Evaluate Timing and Distribution of Rainfall-Induced Shallow Landslides. *ISPRS International Journal of Geo-Information*2023. <https://doi.org/10.3390/ijgi12030105>.
43. Sun Y, Yang K, Hu R, Wang G, Lv J. Model Test and Numerical Simulation of Slope Instability Process Induced by Rainfall. *Water*2022. <https://doi.org/10.3390/w14243997>.
44. Committee Ps. Assessing the current situation, causes and proposing solutions to prevent landslides and local flooding in Lam Dong province. Lam Dong Province, Vietnam: People’s Committee of Lam Dong Province; 2023.
45. DARD. Annual report of Department of Agriculture and Rural Development of Lam Dong Province. Annual report2023.
46. Vakhshoori V, Zare M. Landslide susceptibility mapping by comparing weight of evidence, fuzzy logic, and frequency ratio methods. *Geomatics, Natural Hazards and Risk* 2016;7:1731-52. <https://doi.org/10.1080/19475705.2016.1144655>.
47. Krkač M, Bernat Gazibara S, Sinčić M, Lukačić H, Šarić G, Mihalić Arbanas S. Impact of Input Data on the Quality of the Landslide Susceptibility Large-Scale Maps: A Case Study from NW Croatia. In: Alcántara-Ayala I, Arbanas Ž, Cuomo S, Huntley D, Konagai K, Mihalić Arbanas S, et al., editors. *Progress in Landslide Research and Technology, Volume 2 Issue 1, 2023*. Cham: Springer Nature Switzerland; 2023. p. 135-46. [https://doi.org/10.1007/978-3-031-39012-8\\_4](https://doi.org/10.1007/978-3-031-39012-8_4).
48. Gopinathan P, Nandini CV, Parthiban S, Sathish S, Singh AK, Singh PK. A geo-spatial approach to perceive the groundwater regime of hard rock terrain- a case study from Morappur area, Dharmapuri district, South India. *Groundwater for Sustainable Development* 2020;10:100316. <https://doi.org/10.1016/j.gsd.2019.100316>.

49. Liu H, Mao Z, Wang Y, Kim JH, Bourrier F, Mohamed A, et al. Slow recovery from soil disturbance increases susceptibility of high elevation forests to landslides. *Forest Ecology and Management* 2021;485:118891. <https://doi.org/10.1016/j.foreco.2020.118891>.
50. Thi Ngo PT, Panahi M, Khosravi K, Ghorbanzadeh O, Kariminejad N, Cerda A, et al. Evaluation of deep learning algorithms for national scale landslide susceptibility mapping of Iran. *Geoscience Frontiers* 2021;12:505-19. <https://doi.org/10.1016/j.gsf.2020.06.013>.
51. Dunkerley DL. Light and low-intensity rainfalls: A review of their classification, occurrence, and importance in landsurface, ecological and environmental processes. *Earth-Science Reviews* 2021;214:103529. <https://doi.org/10.1016/j.earscirev.2021.103529>.
52. Addis A. Landslide Susceptibility Mapping Using GIS and Bivariate Statistical Models in Chemoga Watershed, Ethiopia. *Advances in Civil Engineering* 2024;2024:6616269. <https://doi.org/10.1155/2024/6616269>.
53. Shahabi H, Ahmadi R, Alizadeh M, Hashim M, Al-Ansari N, Shirzadi A, et al. Landslide Susceptibility Mapping in a Mountainous Area Using Machine Learning Algorithms. *Remote Sensing* 2023. <https://doi.org/10.3390/rs15123112>.
54. Asmare D. Application and validation of AHP and FR methods for landslide susceptibility mapping around choke mountain, northwestern ethiopia. *Scientific African* 2023;19:e01470. <https://doi.org/10.1016/j.sciaf.2022.e01470>.
55. Nguyen TV. A review on landslide susceptibility mapping methods: Needs and challenges. *Journal of Transportation Science and Technology* 2024;13:1-16. [https://www.doi.org/10.55228/JTST.13\(6\).1-16](https://www.doi.org/10.55228/JTST.13(6).1-16).
56. Huang S, Chen L. Landslide susceptibility mapping using an integration of different statistical models for the 2015 Nepal earthquake in Tibet. *Geomatics, Natural Hazards and Risk* 2024;15:2396908. [10.1080/19475705.2024.2396908](https://doi.org/10.1080/19475705.2024.2396908).
57. Pappas IO, Woodside AG. Fuzzy-set Qualitative Comparative Analysis (fsQCA): Guidelines for research practice in Information Systems and marketing. *International Journal of Information Management* 2021;58:102310. <https://doi.org/10.1016/j.ijinfomgt.2021.102310>.
58. Jibson RW. Debris flows in southern Puerto Rico. 1989.
59. Lumb P. Slope failures in Hong Kong. *Quarterly Journal of Engineering Geology Hydrogeology* 1975;8:31-65.
60. Bhandari R, Senanayake K, Thayalan N. Pitfalls in the prediction on landslide through rainfall data. *International symposium on landslides* 1992. p. 887-90.
61. Endo T. Probable distribution of the amount of rainfall causing landslides. 1970.